

# Navigation Positioning Algorithm for Underwater Gliders in Three-Dimensional Space

Jie Sun<sup>\*†</sup>, Jiancheng Yu<sup>\*</sup>, Aiqun Zhang<sup>\*</sup> and Fumin Zhang<sup>‡</sup>

<sup>\*</sup>Shenyang Institute of Automation, Chinese Academy of Sciences  
Shenyang, 110016, P.R.China.

Email: {sunjie,yjc,zaq}@sia.cn

<sup>†</sup>University of Chinese Academy of Sciences  
Beijing, 100049, P.R.China.

<sup>‡</sup>School of Electrical and Computer Engineering, Georgia Institute of Technology  
Atlanta, Georgia 30332, USA

Email: fumin@gatech.edu

**Abstract**—This paper studies the simultaneous localization and mapping (SLAM) algorithm based on the extended Kalman filter (EKF-SLAM) to achieve the navigation positioning of underwater gliders in the three-dimensional space, as well as to estimate the position of acoustic beacons which are used to measure distances as gliders move. The model of SLAM system consists of two parts: one part is the glider model, calculating the three-dimensional kinematic characteristics of the glider, expanding with the current velocity, and the other part is the beacon model, in order to reckon the planar coordinates of three acoustic beacons without a prior known positions. Based on measurements of distances between the glider and beacons, the position of glider and beacons can be estimated synchronously, utilizing the EKF method. Since the glider runs more than one cycle, the estimation of states in EKF-SLAM system can be optimized, combining with measured location of the glider at the sea surface gained by the global positioning system (GPS). The simulation results indicate that the EKF-SLAM algorithm for glider positioning is correct and effective, which also has high location accuracy.

## I. INTRODUCTION

Underwater gliders [1–3] are a new type of underwater robots which combines buoy technique with Autonomous Underwater Vehicles (AUVs), and completes positioning, data transmission and order reception at the sea surface using the global positioning system (GPS). While gliding through water columns, gliders measure depth and angles through the depth meter and electronic compass, but there is no way to gain the horizontal coordinates of gliders directly, which can impact the effective application of glider measurements. For instance, as mobile platform, gliders can carry sensors to do surveying and mapping, such as two-dimensional distribution of temperature and salinity field [4] or sound intensity field [5, 6] varying with depth-time or depth-distance dimensions, but it is difficult to get three-dimensional distribution of observations with high accuracy. The key to the question is the navigation positioning of underwater gliders in 3D space.

Several research results have been reported on underwater glider localization. In [7], by processing the experimental data of the PhilSea10 Experiment, the estimating uncertainty

in subsurface glider position using transmissions from fixed acoustic sources is acquired to localize the glider, and the algorithm adopted is the least square method (LSM) which is unable to combine the glider moving properties into the localization issue. In order to reduce the error of position estimation, the estimation of glider speed is incorporated into the procedure [8], but there is still an indispensable assumption, that is, the glider remains stationary when the glider receives acoustic signals emitted from sources, while in reality, gliders move continuously in the underwater environment. According to the actual situation, utilizing the method of the extended Kalman filter (EKF), the estimation of glider position can be achieved based on the distances ranging from seabed acoustic beacons to the glider [9, 10]. Whether the LSM or the EKF method used in the glider positioning in the references mentioned above, there is a common premise, that is, the location of acoustic sources or beacons need to be known a priori, which may not be feasible in real life situation. In this paper, the technology of simultaneous localization and mapping (SLAM) is introduced, regarding acoustic beacons as environment characteristics, to estimate the position of glider and beacons synchronously without a prior known positions of beacons.

Although the SLAM algorithm based on the EKF method (EKF-SLAM) has been widely applied to AUVs navigation positioning [11–16], gliders are quite different from conventional AUVs. The glider [3, 17] has neither cameras or imaging sonar which can identify environmental information, nor an inertial navigation system (INS) which can realize the simultaneous localization of the glider and environment characteristics. Thus, the mechanism for the glider localization differs from AUV positioning, even though both utilize the EKF-SLAM algorithm.

This paper establishes a system model for the glider navigation positioning in the three-dimensional space, corrects the position of acoustic beacons using measured location data of the glider at the sea surface gained by GPS, and estimates the position of glider and beacons synchronously, utilizing measurements of the EKF-SLAM based system. The simulation results indicate that the EKF-SLAM algorithm on gliders navigation positioning is correct and effective, which also has high positional accuracy.

---

This work is supported by the National Natural Science Foundation of China (Grant No. 61233013) and the State Key Laboratory of Robotics at Shenyang Institute of Automation (Grant No. 2014-Z02).

## II. POSITIONING SYSTEM STATEMENT

In the practical application of underwater gliders, the principle ways in gliders localization are using GPS at the sea surface, and reckoning the subsurface positions. However, the positioning results under the water are roughly estimated with low accuracy, which may have a significant impact on mapping the distribution of glider measurements in 3D space. Therefore, it is necessary to locate gliders through some more precise method. Different from the methods applied in [7–11], we establish a system with two important parts, the glider and three acoustic beacons. The glider used in this system is equipped with a self-contained hydrophone, which can receive acoustic signals emitted by the acoustic beacons and keep a record. The acoustic beacons, which do not have a prior known positions, are put on the seabed with a certain spatial distribution and emit acoustic signals.

There are three measurements in the positioning system, the distance from the glider to acoustic beacons, the depth of the glider and the heading angle of the glider, in which the ranging component is acquired by means of multiplying transmission time of emission signals by the water sound velocity. Since the glider moves without a break in the underwater environment, distance component of the system measurements should be issued in a round-robin fashion, which means only one ranging result corresponding to a certain acoustic beacon is acquired at a discrete point in time, and the distance measured from each beacon is updated every cycle. Notice that, if the glider is at the sea surface, measured positions of the glider gained by GPS should be added to the system measurements, which is vital to the localization of the acoustic beacons. Through modeling the proposed positioning system, we will describe the system model in the next section.

## III. EKF-SLAM BASED POSITIONING SYSTEM MODELING

On the basis of the positioning system mentioned above, we construct system model, which obviously contains two parts, the glider model and the beacon model. Using the system model, we can roughly estimate the positions of the glider and acoustic beacons. Combining with measurements of the system which is specifically described in the above section, the poorly estimated results can be corrected constantly. Thus, we can estimate the locations of the glider and beacons simultaneously. This is the mechanism of the SLAM based positioning system in this paper.

Taking into account the consecutive motion of the glider under the water, we use EKF to estimate the state of the system, namely the EKF-SLAM algorithm. This algorithm has the ability to process the range measurements individually, as they become available, and to estimate the position of the glider and beacons synchronously.

### A. Positioning System Modeling

As mentioned above, due to three acoustic beacons without a prior known locations, we need to establish both the glider model and the beacon model. Finally, we combine the two models to construct the model of the whole SLAM based positioning system.

1) *Glider model*: Since the glider is not equipped with velocity sensors, such as DVL (Doppler Velocity Log) and ADCP (Acoustic Doppler Current Profiler), the velocity of the glider or the current velocity cannot be measured directly. On account of this limitation, expanding the glider model with current velocity, both the flow-relative velocity of the glider and the current velocity are assumed to be constants, and the current is assumed as layered horizontal flow. The state vector of the glider can be represented by

$$x_g = (x_E, y_N, d, \varphi, v_a, v_x, v_y)^T$$

satisfying the following kinematical equation

$$\begin{bmatrix} \dot{x}_E(t) \\ \dot{y}_N(t) \\ \dot{d}(t) \\ \dot{\varphi}(t) \\ \dot{v}_a(t) \\ \dot{v}_x(t) \\ \dot{v}_y(t) \end{bmatrix} = \begin{bmatrix} v_a \cos \sigma(t) \sin \varphi(t) + v_x \\ v_a \cos \sigma(t) \cos \varphi(t) + v_y \\ v_a \sin \sigma(t) \\ r(t) \\ 0 \\ 0 \\ 0 \end{bmatrix} \quad (1)$$

where  $(x_E, y_N, d)^T$  are the spatial position coordinates of the glider, in which  $x_E$  and  $y_N$  are the East and North components in the planar coordinate system and  $d$  is the depth component,  $\varphi(t)$  is the heading angle of the glider with respect to North,  $v_a$  is the flow-relative velocity of the glider,  $v_x$  and  $v_y$  are the East and North components of the current velocity vector, and  $[r(t), \sigma(t)]$  is the input control, in which  $r(t)$  is the turn rate of the glider and  $\sigma(t)$  is the gliding angle. In this model, the velocities  $v_a, v_x, v_y$  are treated as states without active control. Although the flow is actually intricate time-varying and space-varying, we reduce the complexity of the model in order to study on the nature of the glider positioning problem, which means we consider that  $v_a$  is a constant, and  $v_x$  and  $v_y$  are constants only related to the depth. In our future work, we will add the varying flow to the model.

For the estimation of the model state, if only we provide this glider model with a set of random initial states and the input control, the glider model can reckon the system states at any future time. Nevertheless, the accuracy of the estimated results can be very low if the given initial states greatly deviated from the real values. Therefore, it is necessary to correct the roughly estimated results through measurements.

2) *Beacon model*: On the seabed, three acoustic beacons can be installed with a certain spatial distribution, and the depth of each beacon is assumed to be known and equal to  $b_z$ , without a prior knowledge of the plane coordinates. Since the number of acoustic beacons is known, the state vector of the beacons can be written as

$$x_b = (b_1, b_2, b_3)^T$$

We presume that the acoustic beacons keep still during the experiment or simulation, satisfying the equation,

$$\begin{bmatrix} \dot{b}_1(t) \\ \dot{b}_2(t) \\ \dot{b}_3(t) \end{bmatrix} = \begin{bmatrix} 0 \\ 0 \\ 0 \end{bmatrix} \quad (2)$$

where each position component,  $b_i = (b_{i,x}, b_{i,y})^T$ , ( $i = 1, 2, 3$ ), is the planar position coordinates of each acoustic beacon, in which  $b_{i,x}$  and  $b_{i,y}$  are the East and North components, respectively.

In this model, the planar position coordinates of acoustic beacons at any time are equal to the initial values which are rarely the real case, meaning that there is no way to correct the planar locations of beacons only by means of this beacon model. We need to use measurements in a real-world situation to revise the model output.

3) *SLAM based system modeling*: Considering that the distance between the glider and acoustic beacons is one of the measurements, and the measured location of the glider at the sea surface gained by GPS is crucial to the positioning of acoustic beacons, we combine the glider model and the beacon model to compose the whole positioning system model, which can be called the SLAM system, meaning that the positions of the glider and acoustic beacons can be estimated synchronously.

The state vector of SLAM system is composed of the glider state and beacons state,

$$x = (x_g, x_b)^T$$

Synthesizing the model 1 and 2, the state equation of the SLAM system is

$$\dot{x}(t) = f(x(t), r(t), \sigma(t)) + w(t) \quad (3)$$

where  $w(t)$  is the process noise. Based on the system model, we can roughly estimate the system state, which is prepared for state estimation combining with system measurements.

At discrete points in time,  $t = t_k, (k = 1, 2, 3, \dots)$ , the system measurements,  $\tilde{y}_k = (\tilde{R}_k, \tilde{d}_k, \tilde{\varphi}_k)^T$ , are available as defined by the measuring equation,

$$\tilde{y}_k = h(x_k) + v_k \quad (4)$$

where  $v_k$  is the measurement noise, and  $h(x_k)$  is the measured output of the system corresponding to the true value of the state vector, including three components, namely the range of the glider from one acoustic beacon  $R_k$ , the glider depth  $d_k$ , and the heading angle  $\varphi_k$ , in which the range component is defined as

$$R_k = \left( (x_E(t_k) - b_{i,x}(t_k))^2 + (y_N(t_k) - b_{i,y}(t_k))^2 + (d(t_k) - b_z)^2 \right)^{\frac{1}{2}} \quad (5)$$

It needs to be emphasized that when the glider is at the sea surface, the location of the glider measured by GPS should be added to system measurements. Here we assume that the glider keeps moving from the surface to the subsurface water, which is rarely the case in practice, but this processing can simplify the positioning system with trivial influence on system feasibility. From the above mentioned, system measurements at the surface consist of three components,  $(\tilde{x}_E, \tilde{y}_N, 0)^T$ , or six components,  $(\tilde{R}_k, \tilde{d}_k, \tilde{\varphi}_k, \tilde{x}_E, \tilde{y}_N)^T$ .

Since the state estimated from system model and the system measurements are known, the last question is utilizing the two parts to obtain the optimal results of estimated states. This paper uses EKF, the dynamic filter, to achieve the estimation of the SLAM system.

## B. EKF-SLAM for Underwater Glider Positioning

Since EKF operates recursively on noisy input data to produce a statistically optimal estimate of the system state [18], the SLAM system is based on EKF to estimate the positions of the underwater glider and other states.

Firstly, both the process noise and the measurement noise are assumed to be zero-mean, Gaussian and white, namely  $w(t) \sim N(0, Q(t))$  and  $v_k \sim N(0, R_k)$ .

Secondly, according to the dynamic characteristics of the glider, the system state is estimated by (3) when no measurements can be acquired, while at discrete points in time,  $t = t_k, (k = 1, 2, 3, \dots)$ , the state can be updated by

$$\hat{x}_k^+ = \hat{x}_k^- + K_k (\tilde{y}_k - h(\hat{x}_k^-)) \quad (6)$$

where  $\hat{x}_k^-$  is the state estimated by (3),  $K_k$  is the gain matrix, and  $\hat{x}_k^+$  is the preliminary optimization estimation of the system state with a minimum mean-square error.

Finally, because a self-contained hydrophone is installed on the glider and the full data set is available for post-processing, it is feasible to use the RTS (Rauch-Tung-Striebel) smoothing method [19–21] which integrates the system dynamics in reverse time with a correction term defined as the difference between the preliminary state estimate,  $\hat{x}_f(t)$ , and the smoothed state estimate,  $\hat{x}(t)$ . The smoothed state estimates can be obtained by integration in reverse time

$$\frac{d}{d\tau} \hat{x}(t) = -[F(\hat{x}_f(t)) + K(t)][\hat{x}(t) - \hat{x}_f(t)] - f(\hat{x}_f(t), r(t), \sigma(t)), \hat{x}(T) = \hat{x}_f(T) \quad (7)$$

where  $T$  is the entire time interval,  $\tau = T - t$  is the reverse time,  $K(t)$  is the RTS smoother gain, and  $F(\hat{x}_f(t))$  is defined as

$$F(\hat{x}_f(t)) \equiv \left. \frac{\partial f(\hat{x}_f(t), r(t), \sigma(t))}{\partial x} \right|_{\hat{x}_f(t)} \quad (8)$$

Based on the principle of the RTS smoother, using measurements of all future and past times, it indicates that the RTS smoothing method can improve the estimation accuracy of the positioning system state.

## IV. SIMULATION ANALYSIS

The positioning system described by (3) and (4) was simulated on a computer. Fig. 1 shows the simulation environment: the depth of the water was one hundred meters, the current was assumed as the time-invariant layered horizontal flow, and there were three acoustic beacons on the seabed, constituting an equilateral triangle with 1732 meters of the side length. The schematic diagram of the current direction and the boundary depth of each layer is included in Fig. 1, also the positions of acoustic beacons which are labeled with red dot.

The true values of state variables were given as follows: the first four components of the state vector, the positions of the glider and the heading angle, were real-time varying, and at the initial time, the glider location was set as the origin of coordinates, and the heading angle,  $\varphi|_{t=0}$ , was set as  $-10^\circ$ ; other components of the state vector were all constant values, and the concrete contents were that  $v_a$  was  $0.5m/s$ , values of  $(v_x, v_y)$  was layered in the vertical direction, namely  $(-0.26, -0.15)$



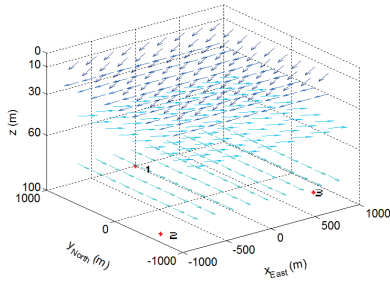


Fig. 1. The simulation environment. Vector shapes indicate the current direction of each layer, and the values of z axis represent the boundary depth of each layer. Three red points are the acoustic beacons.

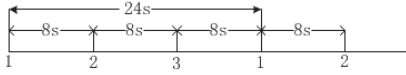


Fig. 2. The schematic diagram of access to measurements. Acquire a measurement every 8 seconds, and update the distance measured from each acoustic beacons every 24 seconds.

on the first floor,  $(-0.25, 0)$  on the second floor,  $(0.17, -0.1)$  on the third floor, and  $(0, -0.2)$  on the fourth floor, and the planar coordinates of three acoustic beacons,  $(b_{i,x}, b_{i,y})(m)$ , were  $(0, 1000)$ ,  $(-866, -500)$ ,  $(866, -500)$ . But all these real values are not known a prior except for the system measurements, we gave a set of random initial state values,

$$\hat{x}_0 = (x_E, y_N, d, \varphi, v_a, v_x, v_y, b_{1,x}, b_{1,y}, b_{2,x}, b_{2,y}, b_{3,x}, b_{3,y})^T \Big|_{t=0} \\ = (0, 0, 0, -10^\circ, 0.3m/s, 0, 0, 5, 1005, -870, -506, 870, -455)^T$$

The choice of the state values, either the real values or initial values, is not limited to the case given above. The current vector of each layer can be set in any direction with any reasonable magnitude, which has trivial effect on the efficiency of the algorithm. The side length of the equilateral triangle composed of acoustic beacons is set according to the range of glider motion, and the influence of length variation is unobvious for the positional accuracy as long as distances between the glider and three acoustic beacons are not approximately equal to each other most of the time.

The simulation experiment was set as follows. Simulation time was 103 minutes, corresponding to six cycles of the glider motion. The glider obtained measurements from the initial time to the end time with the time interval of eight seconds, and once the glider arrived at the sea surface, the measured location of the glider was acquired by GPS. The ranging results were gained in a round-robin fashion, as shown in Fig. 2, which meant the distance measured from each beacons was updated every 24 seconds. In the process of simulation, the measurements were obtained from the true model output with the addition of normally distributed measurement noise. Each element in the covariance matrix of the process noise and the measurement noise was  $2.5 \times 10^{-5}$ . Formally justified in [22], the weight value of the two covariance matrixes represents different degrees of confidence between the system model and the measurements.

The input control of the system is  $[r(t), \sigma(t)]$ . The turn rate,  $r(t)$ , controls the motion model of the glider: if  $r(t)$

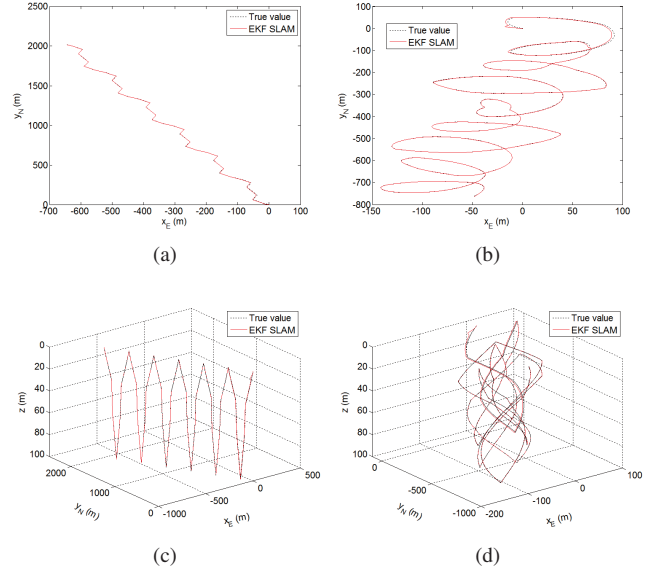


Fig. 3. The moving trajectory of different glider motion model, the linear sawtooth motion in (a) and (c), and the spiraling motion in (b) and (d), corresponding to  $r = 0.5^\circ/s$ . The horizontal projections of two moving trajectory are show in (a)-(b), and (c)-(d) show the three-dimensional positions of the glider under the two movement patterns.

equals to zero, the glider conducts the linear sawtooth motion which is shown in Fig. 3(c), and if not, the glider conducts the spiraling motion, which can be seen in Fig. 3(d) corresponding to  $r = 0.5^\circ/s$ . The gliding angle,  $\sigma(t)$ , represents the nose-down or nose-up motion, and is positive nose-down, in which case the absolute value is equal to that of the nose-up one:  $|\sigma| = 23^\circ$ . Because of the influence of flow, neither the horizontal projection of the sawtooth motion, Fig. 3(a), nor that of the turning motion, Fig. 3(b), is the same as the pattern in still water, which shall be a straight line or a circle. Through the simulation, we found that either the sawtooth or the spiraling motion had the same phenomenon, hence we took the sawtooth motion for example, and analyzed the results specifically.

In order to evaluate the accuracy of state estimates, we need to compare the estimated results with true values. Fig. 4(a) shows the estimation errors of the glider three-dimensional coordinates,  $(x_E - \hat{x}_E), (y_N - \hat{y}_N)$  and  $(z - \hat{z})$ , and the planar coordinates estimation errors of three acoustic beacons,  $(b_{i,x} - \hat{b}_{i,x})$  and  $(b_{i,y} - \hat{b}_{i,y}), (i = 1, 2, 3)$ , are shown in Fig. 4(b). As can be seen from the figure, estimation errors are relatively large during the first cycle, and, with the acquirement of measured location of the glider at the sea surface gained by GPS, the errors converge rapidly in proximity to zero. From Fig. 5, the estimation results of three velocity components are consistent with true values. From the simulation results, the effectiveness of the proposed positioning system using EKF-SLAM algorithm can be verified.

Estimation results obtained from the proposed EKF-SLAM algorithm are compared with the EKF ones [9, 10], which can further demonstrate the correctness and effectiveness of the proposed positioning system based on EKF-SLAM algorithm. TABLE I shows the root-mean-square error (RMSE) of the estimations obtained by EKF-SLAM and EKF, and also the

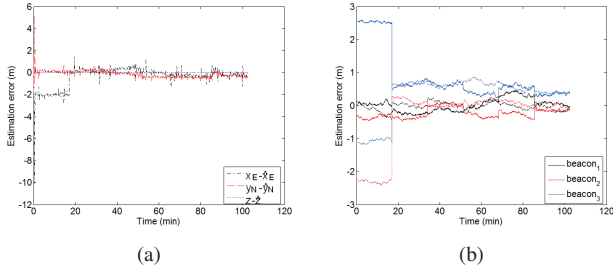


Fig. 4. The estimation errors of the glider and acoustic beacons. Lines of different colors in (a) represent different component of the glider location errors, and in (b) represent the planar position errors of different acoustic beacons. The dash lines and the solid lines in (b) denote the x-direction and y-direction, respectively.

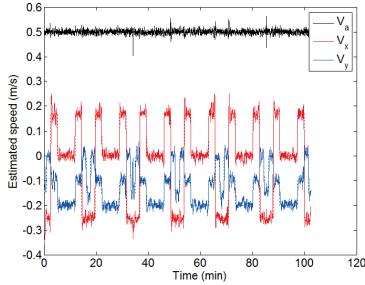


Fig. 5. Comparison between the estimated velocity components and the true values, denoted by solid lines and dash lines.

TABLE I. RMSE OF RESULTS ESTIMATED BY EKF-SLAM AND EKF

RMSE Results	The System States						
	$x_E$ (m)	$y_N$ (m)	$d$ (m)	$\varphi$ (rad)	$v_a$ (m/s)	$v_x$ (m/s)	$v_y$ (m/s)
EKF-SLAM	1.21	0.22	0.01	0.01	0.01	0.03	0.02
EKF	10.1	6.38	0.50	0.31	0.84	1.23	1.53
PD-RMSE	88%	97%	98%	97%	99%	98%	99%
—	$b_{1,x}$ (m)	$b_{1,y}$ (m)	$b_{2,x}$ (m)	$b_{2,y}$ (m)	$b_{3,x}$ (m)	$b_{3,y}$ (m)	—
EKF-SLAM	0.17	0.18	0.93	0.18	0.67	1.13	—
EKF	5	5	4	6	4	5	—
PD-RMSE	97%	96%	77%	97%	83%	77%	—

percent decrease in RMSE (PD-RMSE) between the two methods. Since the planar positions of acoustic beacons are not included in the states of the EKF system, which regards each beacon location as known, the position errors of acoustic beacons are always equal to the initial errors during the entire experiment time. As can be seen, the estimation results gained by the EKF-SLAM method are obviously superior to the results gained by the EKF method because the PD-RMSE outcomes of most estimations are in proximity to one hundred percent.

## V. CONCLUSION AND FUTURE WORK

In this paper, we establish a system model utilizing the EKF-SLAM navigation positioning algorithm to localize the underwater glider in the condition that locations of acoustic beacons are not known a priori. Combining with measured locations of the glider at the sea surface gained by GPS and the other three measurements in the system, positions of the glider and acoustic beacons can be estimated synchronously. The simulation results demonstrate the effectiveness of the EKF-

SLAM based navigation positioning system, and the RMSE of the system states estimated by the EKF-SLAM and EKF are compared with each other, which can further verify the correctness and effectiveness of the EKF-SLAM algorithm for underwater glider positioning in the three-dimensional space.

Since the movement of the glider includes the process of acceleration and deceleration, and ocean currents are time-varying, which can also affect the positions of acoustic beacons, we will optimize the glider model and the beacon model in our future work, in order to approach to the real case.

## ACKNOWLEDGMENT

The authors acknowledge the support of the National Natural Science Foundation of China under Grants 61233013, and the State Key Laboratory of Robotics at Shenyang Institute of Automation under Grants 2014-Z02. The authors would also acknowledge the support for this work provided by the glider research team of the Marine Technology and Equipment Laboratory at Shenyang Institute of Automation, especially Yu Tian and Zhier Chen.

## REFERENCES

- [1] C. C. Eriksen, T. J. Osse, R. D. Light, T. Wen, T. W. Lehman, P. L. Sabin, J. W. Ballard, and A. M. Chiodi, "Seaglider: A long-range autonomous underwater vehicle for oceanographic research," *Oceanic Engineering, IEEE Journal of*, vol. 26, no. 4, pp. 424–436, 2001.
- [2] D. C. Webb, P. J. Simonetti, and C. P. Jones, "Slocum: An underwater glider propelled by environmental energy," *IEEE Journal of Oceanic Engineering*, vol. 26, no. 4, pp. 447–452, 2001.
- [3] J. Yu, F. Zhang, A. Zhang, W. Jin, and Y. Tian, "Motion parameter optimization and sensor scheduling for the sea-wing underwater glider," *Oceanic Engineering, IEEE Journal of*, vol. 38, no. 2, pp. 243–254, 2013.
- [4] L. Uffelen and B. Ma, "Acoustic seaglider deployment cruise report & mid-deployment seaglider status update philippine sea experiment," 2011.
- [5] H. Matsumoto, S. Stalin, R. Embley, J. Haxel, D. Bohnenstiehl, R. Dziak, C. Meinig, J. Resing, and N. Delich, "Hydroacoustics of a submarine eruption in the northeast lau basin using an acoustic glider," in *OCEANS 2010. IEEE*, 2010, pp. 1–6.
- [6] H. Matsumoto, J. H. Haxel, R. P. Dziak, D. R. Bohnenstiehl, and R. W. Embley, "Mapping the sound field of an erupting submarine volcano using an acoustic glider," *The Journal of the Acoustical Society of America*, vol. 129, no. 3, pp. EL94–EL99, 2011.
- [7] L. J. Van Uffelen, E.-M. Nosal, B. M. Howe, G. S. Carter, P. F. Worcester, M. A. Dzieciuch, K. D. Heaney, R. L. Campbell, and P. S. Cross, "Estimating uncertainty in subsurface glider position using transmissions from fixed acoustic tomography sources," *The Journal of the Acoustical Society of America*, vol. 134, no. 4, pp. 3260–3271, 2013.
- [8] L. J. Van Uffelen, B. M. Howe, E.-M. Nosal, G. S. Carter, P. F. Worcester, and M. A. Dzieciuch, "Long-range glider localization using broadband acoustic signals and a linearized model of glider motion."

- [9] L. Techy, K. A. Morgansen, and C. A. Woolsey, "Long-baseline ranging system for acoustic underwater localization of the seaglider underwater glider," Technical report, University of Washington, Aeronautics & Astronautics, Seattle, WA, Tech. Rep., 2010.
- [10] L. Techy, K. Morgansen, and C. Woolsey, "Long-baseline acoustic localization of the seaglider underwater glider," in *American Control Conference (ACC), 2011.* IEEE, 2011, pp. 3990–3995.
- [11] J. J. Leonard and H. F. Durrant-Whyte, "Simultaneous map building and localization for an autonomous mobile robot," in *Intelligent Robots and Systems '91. Intelligence for Mechanical Systems, Proceedings IROS'91. IEEE/RSJ International Workshop on.* IEEE, 1991, pp. 1442–1447.
- [12] R. M. Eustice, "Large-area visually augmented navigation for autonomous underwater vehicles," Ph.D. dissertation, Massachusetts Institute of Technology and Woods Hole Oceanographic Institution, 2005.
- [13] D. Ribas, P. Ridao, J. Neira, and J. D. Tardos, "Slam using an imaging sonar for partially structured underwater environments," in *Intelligent Robots and Systems, 2006 IEEE/RSJ International Conference on.* IEEE, 2006, pp. 5040–5045.
- [14] R. M. Eustice, O. Pizarro, and H. Singh, "Visually augmented navigation for autonomous underwater vehicles," *Oceanic Engineering, IEEE Journal of*, vol. 33, no. 2, pp. 103–122, 2008.
- [15] J. Salvi, Y. Petillot, S. Thomas, and J. Aulinas, "Visual slam for underwater vehicles using video velocity log and natural landmarks," in *OCEANS 2008.* IEEE, 2008, pp. 1–6.
- [16] Y. Wang, K. Liu, and X. Feng, "Optimal auv trajectories for bearings-only tracking," *ROBOT*, vol. 36, no. 2, pp. 179–184, 2014.
- [17] J.-c. Yu, A.-q. Zhang, W.-m. Jin, Q. Chen, Y. Tian, and C.-j. Liu, "Development and experiments of the sea-wing underwater glider," *China Ocean Engineering*, vol. 25, pp. 721–736, 2011.
- [18] R. E. Kalman, "A new approach to linear filtering and prediction problems," *Journal of Fluids Engineering*, vol. 82, no. 1, pp. 35–45, 1960.
- [19] H. E. Rauch, C. Striebel, and F. Tung, "Maximum likelihood estimates of linear dynamic systems," *AIAA journal*, vol. 3, no. 8, pp. 1445–1450, 1965.
- [20] J. L. Crassidis and J. L. Junkins, *Optimal estimation of dynamic systems.* CRC press, 2011.
- [21] G. J. Bierman, "Fixed interval smoothing with discrete measurements," *International Journal of Control*, vol. 18, no. 1, pp. 65–75, 1973.
- [22] D. Simon, *Optimal state estimation: Kalman, H infinity, and nonlinear approaches.* John Wiley & Sons, 2006.